` The Basis for the Distinct Biological Activities of Vascular Endothelial Growth Factor Receptor-1 Ligands

Andrey Anisimov, Veli-Matti Leppänen, Denis Tvorogov, Georgia Zarkada, Michael Jeltsch, Tanja Holopainen, Seppo Kaijalainen and Kari Alitalo (2 July 2013)

Science Signaling **6** (282), ra52. [DOI: 10.1126/scisignal.2003905]

RECEPTOR-LIGAND INTERACTIONS

The Basis for the Distinct Biological Activities of Vascular Endothelial Growth Factor Receptor–1 Ligands

Andrey Anisimov,[1]* Veli-Matti Leppänen,[2]* Denis Tvorogov,[1] Georgia Zarkada,[1,2] Michael Jeltsch,[1,2] Tanja Holopainen,[1] Seppo Kaijalainen,[1] Kari Alitalo[1,2]†

Vascular endothelial growth factors (VEGFs) regulate blood and lymphatic vessel development through VEGF receptors (VEGFRs). The VEGFR immunoglobulin homology domain 2 (D2) is critical for ligand binding, and D3 provides additional interaction sites. VEGF-B and placenta growth factor (PlGF) bind to VEGFR-1 with high affinity, but only PlGF is angiogenic in most tissues. We show that VEGF-B, unlike other VEGFs, did not require D3 interactions for high-affinity binding. VEGF-B with a PlGF-derived L1 loop (B-L1^P) stimulated VEGFR-1 activity, whereas PlGF with a VEGF-B–derived L1 loop (P-L1^B) did not. Unlike P-L1^B and VEGF-B, B-L1^P and PlGF were also angiogenic in mouse skeletal muscle. Furthermore, B-L1^P also bound to VEGFR-2 and activated downstream signaling. These results establish a role for L1-mediated D3 interactions in VEGFR activation in endothelial cells and indicate that VEGF-B is a high-affinity VEGFR-1 ligand that, unlike PlGF, cannot efficiently induce signaling downstream of VEGFR-1.

INTRODUCTION

The growth and maintenance of blood and lymphatic vessels are governed by several receptor tyrosine kinase (RTK) families, among which the vascular endothelial growth factor receptor (VEGFR) family plays a key role. VEGFR-2 is the main receptor that transduces angiogenic signals (*1*, *2*). VEGF-A binds to both VEGFR-1 and VEGFR-2, whereas VEGF-B and placenta growth factor (PlGF) bind only to VEGFR-1 (*3*). VEGFs bind also to neuropilins (Nrp) and heparan sulfate proteoglycans (HSPGs), which act as VEGFR co-receptors (*4*).

Although VEGF-B and PlGF bind to the same receptors, they differ greatly in their biological properties. PlGF induces angiogenesis or arteriogenesis in various in vivo models (*5*, *6*), whereas VEGF-B has weak angiogenic activity in most tissues (*7*). The two ligands show distinct distribution patterns during development; for example, the abundance of PlGF is high in placental trophoblasts, whereas that of VEGF-B is highest in developing cardiac muscle (*8*). Dysregulation of the PlGF/VEGFR-1 axis has been linked to preeclampsia in humans and rats, and transgenic or adenovirus-mediated overexpression of VEGF-B stimulates coronary vasculature development and arterialization in the rat, pig, and rabbit heart (*9*–*12*). However, deletion of either factor from mouse embryos does not interfere with normal vascular development (*13*–*15*).

Gene transfer of VEGF ligands has been tested as a therapeutic tool for peripheral ischemia, and PlGF, but not VEGF-B, induces formation of perfused arterialized microvessels in mouse skeletal muscle (*9*). The accelerated growth of mouse tumors overexpressing a transfected PlGF construct requires the tyrosine kinase activity of VEGFR-1 (*16*), and a blocking monoclonal antibody against PlGF has been reported to inhibit the growth of various tumor xenografts (*17*, *18*). However, four other PlGF blocking antibodies have been subsequently reported to be unable to inhibit tumor growth except in rare cases in which the tumor cells were VEGFR-1 positive (*19*, *20*). Unlike PlGF, transgenic expression of VEGF-B retards tumor growth in a mouse model of pancreatic neuroendocrine tumorigenesis (*21*). These studies indicate that, although these ligands bind to the same RTK, VEGFR-1, and to the same co-receptors, Nrp-1 and HSPG, VEGF-B and PlGF have distinct biological functions in several settings.

VEGFRs have seven immunoglobulin (Ig) homology domains in their extracellular region. VEGFR-1 domain 2 (D2) determines VEGF-A and PlGF binding, and crystal structure determination of D2 complexes has established ligand-induced dimerization as a central paradigm for VEGFR activation (*22*–*24*). In addition, residues in VEGFR-1 D3 contribute to high-affinity binding of VEGF-A and PlGF (*23*, *25*). High-affinity VEGF-A binding to VEGFR-2 also depends on D3 (*23*, *26*). VEGF-B shows a similar mode of binding to VEGFR-1 D2 as VEGF-A and PlGF (*27*), but its dependence on D3 has not been studied. Structure determination of the VEGF-C complex with VEGFR-2 ligand-binding domains (D2–3) has defined the distinct roles of the VEGF-family ligand receptor–binding epitopes in loops L1 to L3 and the N-terminal helix (αN) (*28*). In particular, L2 and L3 interact with both D2 and D3, whereas L1 interacts only with D3.

To identify the structural features of VEGF-B and PlGF that are responsible for their distinct biological properties, we designed several VEGF-B/PlGF swap chimeras by exchanging L1 and L3. A similar strategy has been previously used to map the determinants of VEGF-E binding to VEGFR-2 (*29*). We show that the distinct receptor-activating properties of VEGF-B and PlGF can be attributed to differential involvement of L1 in the binding to VEGFR-1. On the basis of our results, we present a model in which D3 interactions are required for productive VEGFR-1 dimerization, tyrosine kinase phosphorylation, and downstream signaling.

RESULTS

Unlike VEGF-B, PlGF stimulates ERK1/2 phosphorylation in vivo

We have previously shown that, unlike VEGF-B, PlGF induces an angiogenic response in mouse skeletal muscle when delivered through recombinant adeno-associated virus (rAAV) (*9*). Here, we performed short-time stimulation experiments in vivo to probe the ability of VEGF-B and PlGF to

[1]Translational Cancer Biology Program, Biomedicum Helsinki and Helsinki University Central Hospital, University of Helsinki, FIN-00014 Helsinki, Finland. [2]Wihuri Research Institute, Biomedicum Helsinki, Haartmaninkatu 8, FIN-00290 Helsinki, Finland.
*These authors contributed equally to this work.
†Corresponding author. E-mail: kari.alitalo@helsinki.fi

stimulate the mitogen-activated protein kinase (MAPK) extracellular signal–regulated kinases 1 and 2 (ERK1/2) as one of the major pathways leading to endothelial proliferation. To improve the expression and secretion of the mouse VEGF-B construct, we generated an N-glycosylation site with a Q96N/R98T double mutation, which mimicked the conserved glycosylation site in PlGF and other VEGF family members. Purified recombinant VEGF-B or PlGF was injected into the tail vein, and phosphorylation of ERK1/2 was analyzed in total heart lysates. Under these conditions, only PlGF induced phosphorylation of ERK1/2 (Fig. 1, A and B). To exclude nonspecific effects in this experiment, we used only the VEGF-B and PlGF receptor-binding domains encoded by exons 1 to 5 and excluded the Nrp and HSPG binding regions (Fig. 1, C and D).

High-affinity binding of PlGF, but not VEGF-B, to VEGFR-1 is D3-dependent

To compare VEGF-B and PlGF binding to VEGFR-1, we also purified VEGFR-1 domains D1–2 and D1–3 produced in insect cells. We used isothermal titration calorimetry (ITC) for the thermodynamic characterization of the enthalpy (ΔH), entropy (ΔS), and affinity [dissociation constant (K_D)] of the binding. Enthalpy and entropy both contribute to the free energy (ΔG) of binding ($\Delta G = \Delta H - T\Delta S$). The data confirmed the 2:2 ligand/receptor stoichiometry and showed that the binding is enthalpically (negative ΔH) and entropically (positive ΔS) favorable. Consistent with previously published results (*23*), the presence of D3 increased the affinity of PlGF for VEGFR-1. The presence of D3 was also associated with a large change in enthalpy of PlGF binding, suggesting that D3 provides additional ionic interactions (Fig. 1, E and F). VEGF-B showed high-affinity binding to both VEGFR-1 D1–2 and D1–3, and in comparison to PlGF binding, VEGF-B binding to D1–2 and D1–3 revealed a smaller change in enthalpy (Fig. 1, F and G). Thus, the ITC titrations revealed a major difference between PlGF and VEGF-B in the requirement for D3 in binding to VEGFR-1. Construction of a homology model based on VEGF-A binding to VEGFR-2 suggested that PlGF loop L1 or L3 or both were involved in the D3 interactions (Fig. 1H).

PlGF L1 is critical for VEGFR-1 activation

To further analyze the contribution of the different loops to VEGFR-1 binding and stimulation, we designed a set of L1 and L3 swap chimeras using

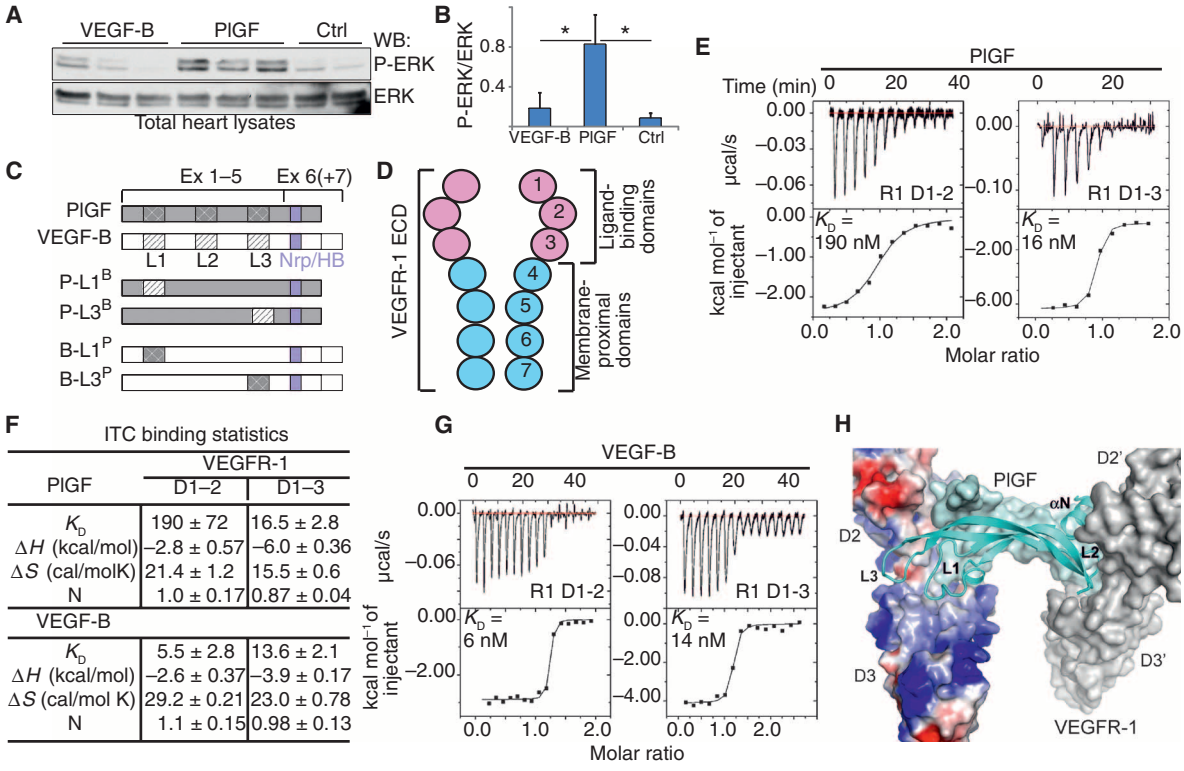

Fig. 1. VEGF-B and PlGF differ in their interaction with VEGFR-1. (**A**) Analysis of ERK1/2 phosphorylation in mouse heart after stimulation with the indicated ligands. Three mice were used in each treatment group. (**B**) Densitometric analysis of the protein bands. $n = 3$ mice for each treatment group. $^*P < 0.05$. Data are representative of at least three independent experiments. (**C**) Schematic structures of PlGF and VEGF-B and the various chimeras. Ex, exon; Nrp, neuropilin-binding domain; HB, heparin-binding domain. (**D**) Schematic representation of the VEGFR-1 extracellular domain (ECD) and ligand-binding domains 1 to 2 (R1 D1–2) and domains 1 to 3 (R1 D1–3) used for the binding studies. (**E**) Isothermal calorimetric (ITC) titration of PlGF binding to VEGFR-1 D1–2 and VEGFR 1 D1–3. Representative plots of three independent measurements are shown. (**F**) Summary of the enthalpy change (ΔH), entropy change (ΔS), binding affinities (K_D), and stoichiometry (N) from the ITC binding experiments. Data are means ± SD. (**G**) ITC titration of VEGF-B (exons 1 to 5) binding to VEGFR-1 D1–2 and VEGFR-1 D1–3. Representative plots of three independent measurements are shown. (**H**) A homology model of PlGF in complex with VEGFR-1 D2–3 based on the crystal structures of PlGF/VEGFR-1 D2 and VEGF-A/VEGFR-2 D2–3 complexes (PDB codes 1RV6 and 3V2A, respectively). PlGF is colored in cyan and shown as a cartoon model. VEGFR-1 D2–3 is shown as a surface representation, and one of the chains is colored according to its electrostatic surface potential. Receptor-binding epitopes L1 to L3 and αN of PlGF are marked in the figure.

full-length PlGF and VEGF-B, now including the Nrp and HSPG binding domains. Figure 1C and fig. S1 show schematic alignment of VEGF-B and PlGF, highlighting the swapped loop/domain structures. B-L1^{P} stands for VEGF-B with the PlGF-derived L1, and P-L1^{B} stands for PlGF with the VEGF-B–derived L1. The same principle was used to name the L3-swap chimeras B-L3^{P} and P-L3^{B}. To analyze how the loop swapping affected the binding to VEGFR-1, the proteins expressed in 293T cells were metabolically labeled with ^{35}S–amino acids, precipitated with soluble VEGFR-1–Fc fusion protein, and analyzed by gel electrophoresis. These results indicated that the chimeric proteins retained the binding properties of their parental proteins (Fig. 2A).

We then analyzed whether domain swapping affected the VEGFR-1–stimulating activity of the parental proteins. Proliferation was measured in VEGFR-1/EpoR fusion receptor–expressing BaF3 (VEGFR-1/EpoR-BaF3) cells cultured with conditioned medium from 293T cells transfected with the growth factor constructs. These cells undergo apoptosis in interleukin-3 (IL-3)–deficient medium, but they can be rescued (and continue to proliferate) by the addition of the respective VEGFR ligands (*30*, *31*). As expected, PlGF strongly stimulated VEGFR-1/EpoR-BaF3 cell proliferation, whereas VEGF-B showed little activity in the assay (Fig. 2B and fig. S2A). The activity of the B-L3^{P} chimeric protein corresponded to its parental backbone, and the activity of P-L3^{B} was increased in comparison with PlGF. The L1 swaps in both VEGF-B and PlGF reversed the activities of the parental molecules, so that the resulting chimera B-L1^{P} was converted into a VEGFR-1 activating ligand and P-L1^{B} into an inactive ligand in this assay. We thus focused on the further analysis of these chimeras.

For detailed analysis of receptor binding and signal transduction, we produced and purified VEGF-B, PlGF, B-L1^{P}, and P-L1^{B} (Fig. 2C; see also Fig. 1C for schematics). The purified proteins behaved similarly to their mammalian-derived counterparts in VEGFR-1 binding and in the stimulation of VEGFR-1/EpoR-BaF3 cell proliferation (Fig. 2D and fig. S2B). B-L1^{P} was as active as VEGF-A or PlGF, whereas P-L1^{B} had no activity. VEGF-B showed limited VEGFR-1 activation with maximal stimulation of cell proliferation of only about 30% of that obtained by PlGF, although the dose-response curves of VEGF-B and PlGF were comparable in shape [half-maximal effective concentration (EC_{50}) values were 1.40 ± 0.56 and 0.56 ± 0.14 ng/ml, respectively]. Thus, VEGF-B was less efficient at activating EpoR kinase and downstream signaling of the fusion receptor, suggesting compromised VEGFR-1 dimerization.

To confirm the receptor-stimulating properties in vivo, we injected the recombinant proteins into the tail vein of mice, and we analyzed the tyrosine phosphorylation of VEGFR-1 (Tyr^{1213}) in lung lysates by Western blotting. The results indicated that PlGF and B-L1^{P} stimulated VEGFR-1 (Tyr^{1213}) phosphorylation in vivo to a greater extent than the other tested proteins (Fig. 2, E and F). The relatively weak activity of VEGF-A in this assay could be attributed to its dual receptor specificity or HSPG binding (*1*, *2*, *4*), thus possibly decreasing the availability of the ligand for interaction with VEGFR-1. On the other hand, PlGF has also been reported to stim-

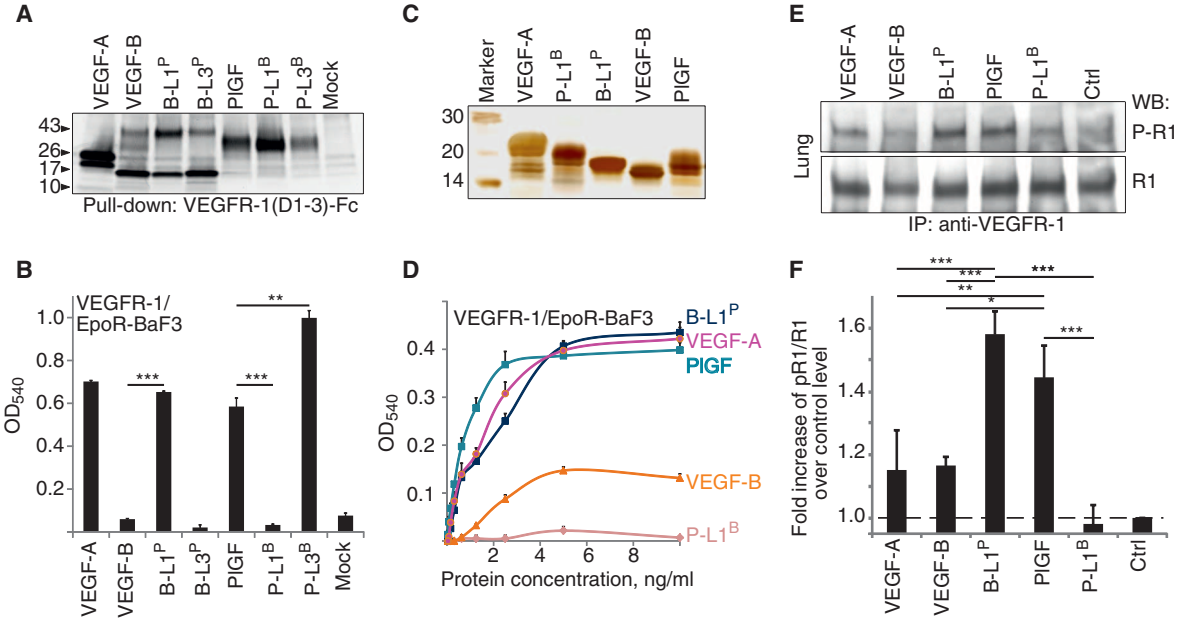

Fig. 2. Ligand L1 mediates differential VEGFR-1 activation. (**A** and **B**) Full-length native and chimeric ligands were produced in 293T cells metabolically labeled with [^{35}S]methionine and analyzed by a pull-down assay using soluble VEGFR-1 (A) or the VEGFR-1/EpoR-BaF3 MTT [3-(4,5-dimethylthiazol-2-yl)-2,5-diphenyltetrazolium bromide] assay (B). Data are representative of three (A) and two (B) independent experiments. Each bar in (B) represents mean ± SD from three technical replicates from one experiment. Data from a separate experiment performed under identical conditions are shown in fig. S2A. (**C**) Purified native and chimeric ligands (exons 1 to 5; see Fig. 1C) produced in the Sf21/baculovirus system, analyzed by SDS–polyacrylamide gel electrophoresis, and silver-stained. (**D**) Analysis of the purified ligands in the VEGFR-1/EpoR-BaF3 MTT assay. Data are representative of three independent experiments. Each dot represents mean ± SD from three technical replicates from a representative experiment. Data from a separate experiment performed under identical conditions are shown in fig. S2B. (**E**) Analysis of VEGFR-1 (Tyr^{1213}) phosphorylation and total VEGFR-1 in mouse lungs after stimulation with purified ligands. Each lane contains tissue sample from a single treated animal. Data are representative of three independent experiments. (**F**) Combined data from densitometric analysis of the protein bands from all three independent experiments. Each bar represents mean ± SD. *P < 0.05; **P < 0.01; ***P < 0.001.

ulate VEGFR-1 tyrosine phosphorylation more strongly than VEGF-A in VEGFR-1–overexpressing endothelial cells in vitro (*32*).

To confirm that the VEGF-B L1 confers inability to activate VEGFR-1, we additionally transplanted it to VEGF-A in place of the native L1. Unlike the parental protein, this mutant (A-L1^{B}) was inactive in the VEGFR-1/EpoR-BaF3 assay, although both proteins bound equally to VEGFR-1 in the pull-down assay (fig. S2, C and D). Together, these findings indicate that L1-mediated interactions are critical for VEGFR-1 activation.

B-L1^{P} is as angiogenic as PlGF in mouse skeletal muscle

To determine how the in vitro activity of the chimeras corresponds to their angiogenic activity profiles in vivo, we used rAAV delivery to express the chimeras in mouse tibialis anterior muscle. In line with the data from the VEGFR-1/EpoR-BaF3 assay, PlGF and B-L1^{P}, but not P-L1^{B} and VEGF-B, stimulated vascular endothelial cell proliferation and smooth muscle cell recruitment by the vessels (Fig. 3, A and B). Because VEGFR-2 is the main angiogenic receptor in mice and humans, we also checked whether VEGFR-2 was activated in response to B-L1^{P} in vivo and used VEGF-A as a positive control. The purified ligands were injected into the tail vein of mice, and phosphorylation of VEGFR-2 was analyzed from lung and heart lysates. B-L1^{P} stimulated VEGFR-2 phosphorylation, although considerably more weakly and at higher concentrations than VEGF-A (Fig. 3C). Titration experiments with doses of VEGF-A and B-L1^{P} that induced similar amounts of VEGFR-2 phosphorylation (2 and 25 μg per mouse, respectively) indicated that VEGF-A and B-L1^{P} induce similar kinetics of VEGFR-2 and ERK1/2 phosphorylation (Fig. 3C). Thus, in addition to its VEGFR-1–stimulating activity, B-L1^{P} can promote an angiogenic response by activating VEGFR-2 tyrosine phosphorylation in vivo.

B-L1^{P} stimulates VEGFR-2 tyrosine phosphorylation and downstream signaling in endothelial cells in vitro

To better understand B-L1^{P}–induced VEGFR-2 activation, we analyzed VEGFR-2 tyrosine phosphorylation in vitro using human umbilical vein endothelial cells (HUVECs). VEGFR-2 (Tyr^{1175}) phosphorylation was stimulated by VEGF-A and B-L1^{P}, but not by PlGF, VEGF-B, or P-L1^{B} (Fig. 4A). We also analyzed ERK1/2 (Thr^{202}/Tyr^{204}) and Akt (Ser^{473}) phosphorylation by Western blotting of HUVEC lysates. Phosphorylation of VEGFR-2 Tyr^{1175} creates a binding site for phospholipase Cγ and for the adapter proteins SHB and Sck (*2*). VEGF-A and B-L1^{P} stimulated the phosphorylation of all three proteins (Fig. 4B). At least part of these signals could also be mediated through VEGFR-1 that is present in the HUVEC cells.

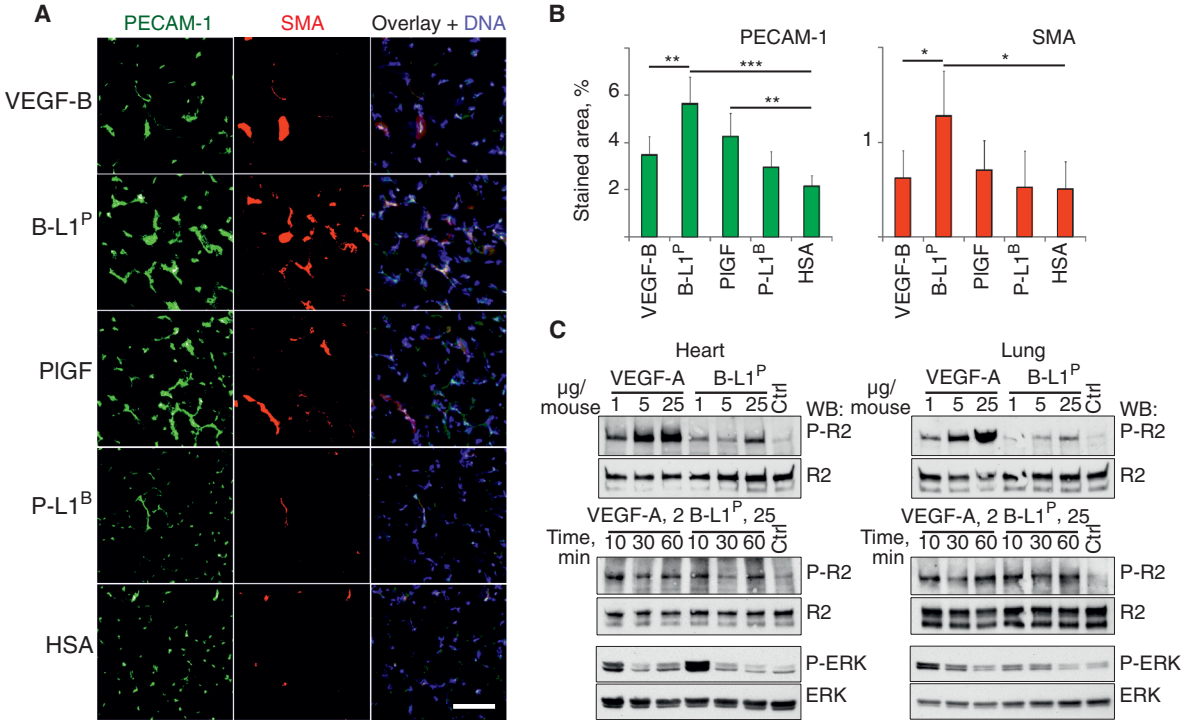

Fig. 3. Analysis of angiogenic activity and in vivo signaling properties of the parental and chimeric proteins. (**A**) Unlike VEGF-B, B-L1^{P} induces endothelial cell proliferation and smooth muscle cell recruitment to mouse skeletal muscle. rAAVs encoding the indicated genes were injected into mouse anterior tibialis muscle. After 2 weeks, isolated muscles were stained for platelet endothelial cell adhesion molecule 1 (PECAM-1) and smooth muscle actin (SMA). Nuclei (DNA) were counterstained with DAPI (4′,6-diamidino-2-phenylindole). Images are representative of two independent experiments. (**B**) Quantification of stained areas in (A). Each bar represents mean ± SD obtained from four or six independently treated muscles (two or three mice in each treatment group). Two sections, with three or four randomly chosen view areas in both, were analyzed from each muscle. $n = 4$ or 6 independent muscle samples. $^{*}P < 0.05$; $^{**}P < 0.01$; $^{***}P < 0.001$. (**C**) B-L1^{P} induces VEGFR-2 (Tyr^{1175}) phosphorylation in mouse heart and lung. VEGF-A or B-L1^{P} was injected into the tail vein and allowed to circulate for 10 min (upper panels for heart and lung P-R2/R2) or for the indicated times (lower panels for P-R2/R2 and P-ERK/ERK). The hearts and lungs were homogenized and analyzed by Western blotting for phospho-VEGFR-2 (Tyr^{1175}) total VEGFR-2, phospho-ERK1/2, and total ERK1/2. Data are representative of two independent experiments.

VEGFR-2 activation by B-L1^P does not require VEGFR-1/VEGFR-2 heterodimers

VEGF-A can homo- and heterodimerize VEGFR-1 and VEGFR-2 and stimulate downstream signaling, but formation of VEGFR-2/VEGFR-2 and VEGFR-1/VEGFR-2 dimers results in distinct signaling patterns (*33*, *34*). Using blood microvascular endothelial cells (BECs) stimulated with purified ligands, we first demonstrated that, unlike VEGF-B and PlGF, VEGF-A and B-L1^P increased the formation of the VEGFR-1/VEGFR-2 heterodimer over baseline (Fig. 4, C and D).

We then analyzed whether B-L1^P could activate VEGFR-2 in the absence of VEGFR-1 to exclude the possibility of a VEGFR-1–to–VEGFR-2 transphosphorylation event. The NIH 3T3 fibroblast cell line was transfected with a retrovirus encoding full-length VEGFR-2 fused to a C-terminal Strep-tag. B-L1^P stimulated tyrosine phosphorylation of the VEGFR-2–Strep-tag protein, although at considerably higher concentrations than VEGF-A, suggesting that B-L1^P has a lower VEGFR-2–binding affinity than VEGF-A. PlGF and VEGF-B were inactive in this assay (Fig. 4E). We additionally confirmed the VEGFR-1–negative phenotype of the VEGFR-2–Strep-tag–expressing NIH 3T3 cell line (Fig. 4F). Furthermore, VEGF-B pretreatment of endothelial cells did not affect phosphorylation of VEGFR-2 or ERK1/2 stimulated by VEGF-A or B-L1^P (Fig. 4G), further confirming that VEGFR-1 is not involved. Similar results were obtained with porcine aortic endothelial (PAE) cells overexpressing VEGFR-2 after retrovirus-mediated transduction (fig. S3).

B-L1^P shows weak binding to VEGFR-2

ITC measurements were used to study the affinity of B-L1^P to VEGFR-1 and VEGFR-2. B-L1^P bound to monomeric VEGFR-1 D1–3 with a K_D

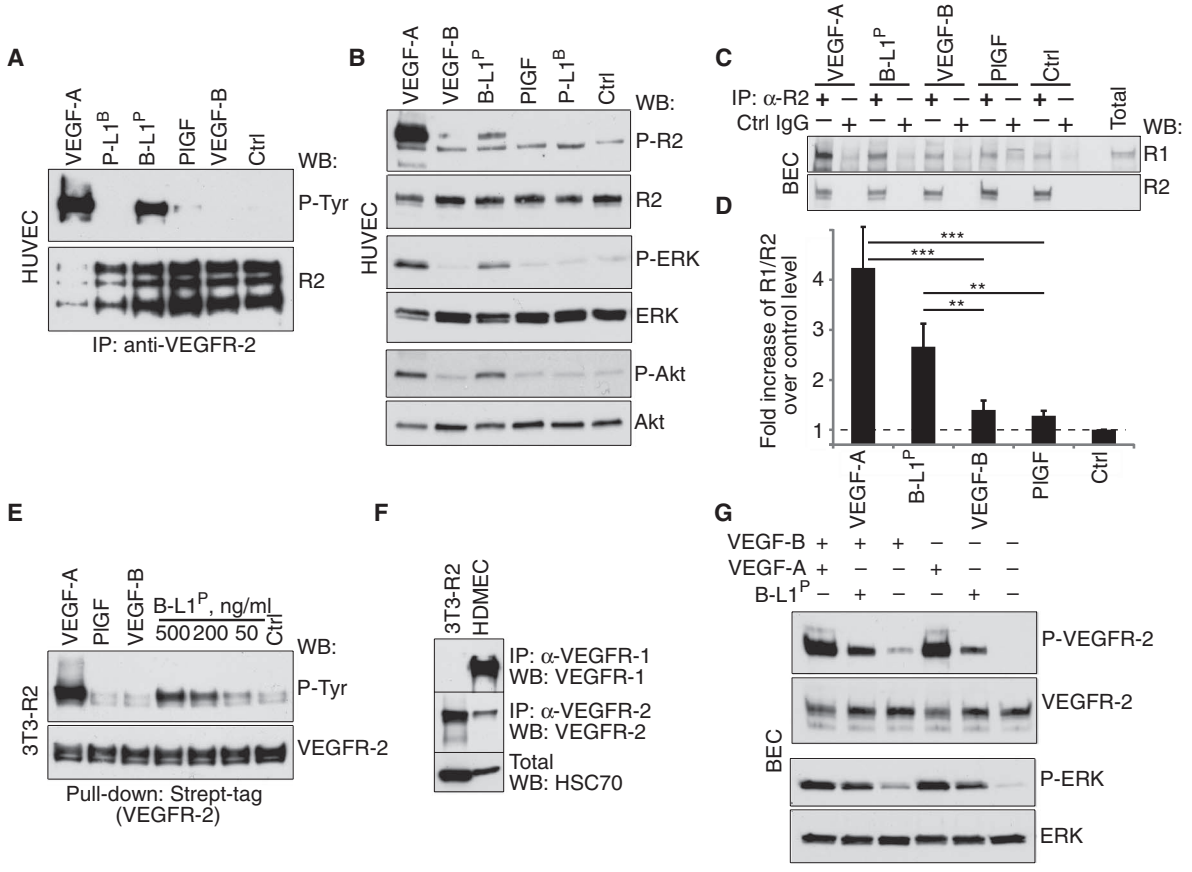

Fig. 4. B-L1^P can activate VEGFR-2. (**A**) Ligand-induced phosphorylation of VEGFR-2. VEGFR-2 precipitates from HUVECs stimulated with the indicated purified ligands were Western-blotted for total phosphotyrosine. (**B**) Ligand-induced phosphorylation of VEGFR-2 (P-R2, Tyr^{1175}), ERK1/2 (Thr^{202}/Tyr^{204}), and Akt (Ser^{473}), analyzed by Western blotting. (**C**) Formation of ligand-induced VEGFR-1/VEGFR-2 heterodimers. BECs were treated with the indicated ligands. VEGFR-2 was precipitated with anti–VEGFR-2 antibody or species-matching IgG (negative control) and analyzed by Western blotting for VEGFR-1. A representative image is shown. Three independent experiments were performed with similar results. (**D**) Averaged data (means ± SEM) from densitometric analysis of the polypeptide bands from three independent heterodimerization experiments, such as the one shown in (C). (**E**) Titration of B-L1^P–induced VEGFR-2 tyrosine phosphorylation. VEGFR-2–Strep-tag was precipitated from NIH 3T3–VEGFR-2–Strep-tag cells stimulated with the indicated ligands, and tyrosine phosphorylation and total VEGFR-2 were analyzed by Western blotting. (**F**) Confirmation that VEGFR-1 is not detected in NIH 3T3–VEGFR-2–Strep-tag cells. The indicated cells were lysed and Western-blotted for VEGFR-1 and VEGFR-2. (**G**) High molar excess of VEGF-B does not inhibit VEGFR-2 phosphorylation induced by B-L1^P or VEGF-A. BECs were preincubated with VEGF-B for 1 min and further stimulated with VEGF-A or B-L1^P for an additional 10 min, and cell lysates were analyzed by Western blotting for phosphorylation of VEGFR-2 (Tyr^{1175}) and ERK1/2. Data are representative of two independent experiments.

of 50.4 ± 21 nM. Titrations with VEGFR-2 D2–3 indicated low-affinity binding, but data fitting was not possible (Fig. 5, A and B). Because B-L1^P and VEGFR-2 D2–3 were not available in concentrations high enough for accurate ITC assays, we performed an enzyme-linked immunosorbent assay (ELISA)–based competition assay to find out whether B-L1^P, VEGF-B, or PlGF, like VEGF-C, can compete with VEGF-A for binding to VEGFR-2. Indeed, the B-L1^P binding to VEGFR-2 had an IC_{50} (half-maximal inhibitory concentration) value of 2.0 ± 0.45 μM, compared to 7.4 ± 1.6 nM for VEGF-C (Fig. 5C).

VEGF-B has a unique L1 structure

The VEGF-B L1 sequence differs from those of VEGF-A and PlGF (fig. S1). Comparison of VEGF-A and PlGF crystal structures in their complexes with VEGFR-1 D2 [Protein Data Bank (PDB) codes 1FLT and 1RV6, respectively] revealed almost identical L1 and L3 conformations between the two (Fig. 5D). Accordingly, the L1 chimeras A-L1^P and P-L1^A retained their parental VEGFR-1/EpoR-BaF3 cell activation and VEGFR-2 stimulation properties in BECs (figs. S2C and S4, A and B). The L1 structure in both VEGF-A and PlGF is dominated by a helical (3_{10}) turn followed by a conserved Glu-Tyr-Pro-x-Glu motif providing multiple, conserved ionic interactions with the rest of the monomer. In the corresponding VEGF-B structure (PDB code 2XAC), L1 lacks the helical turn and the conserved motif along with their interactions (Fig. 5D). Molecular modeling of B-L1^P suggests that PlGF-derived L1 in B-L1^P could accommodate the parental structure, and L1 loop conformation may be stabilized with intramolecular interactions similar to those in PlGF, such as the Glu^{46}-Arg^{56} salt bridge and the Tyr^{47}-Ser^{94} hydrogen bond (PlGF or VEGF-B numbering; Fig. 5D). Also, VEGF-B with the L1 from VEGF-A (B-L1^A) stimulated VEGFR-1/EpoR-BaF3 cells and VEGFR-2 (and ERK1/2) phosphorylation with dose-response kinetics similar to B-L1^P (figs. S2C and S4, A and B).

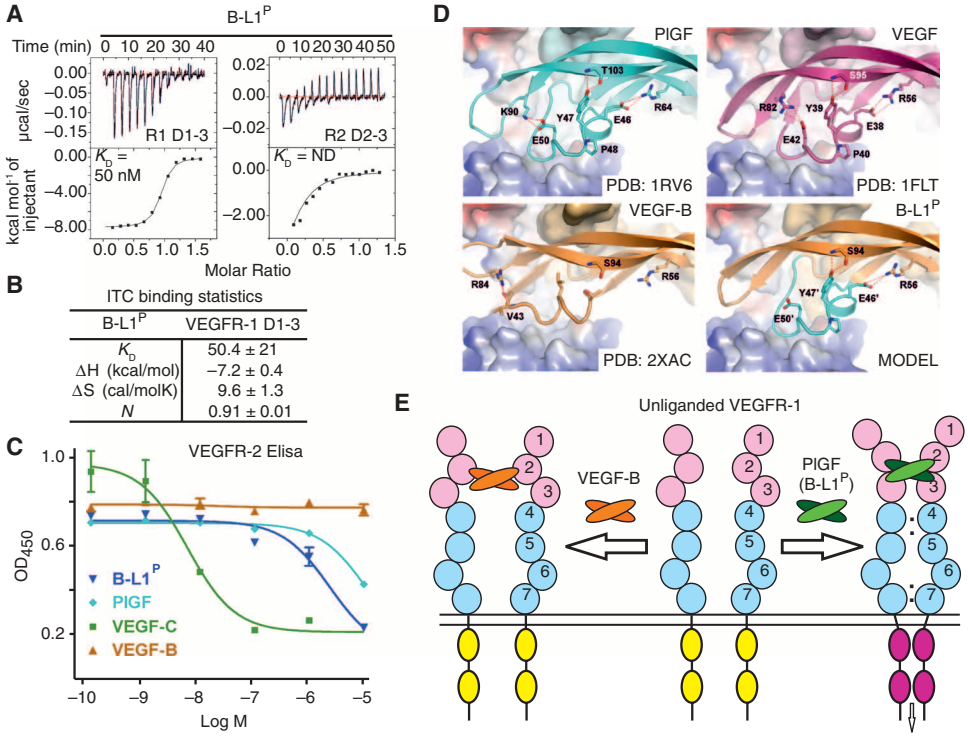

Fig. 5. B-L1^P binds with high affinity to VEGFR-1 but weakly to VEGFR-2. (**A**) Calorimetric titrations of B-L1^P to VEGFR-1 D1–3 (R1 D1–3) and VEGFR-2 D2–3 (R2 D2–3). Representative plots of three independent experiments are shown. ND, not defined. (**B**) Summary of the enthalpy change (Δ*H*), entropy change (Δ*S*), binding affinities (K_D), and stoichiometry (*N*) from the ITC binding experiments, shown in (A). Data are means ± SD (*n* = 3 independent experiments). (**C**) Analysis of B-L1^P binding to VEGFR-2 by an ELISA-based competition assay. Competition of VEGF-A binding to VEGFR-2 by B-L1^P and VEGF-C had IC_{50} values of 2.0 ± 0.45 μM (*n* = 3 independent experiments) and 7.4 ± 1.6 nM (*n* = 3 independent experiments), respectively. The IC_{50} values could not be defined for the competition by PlGF or VEGF-B. (**D**) Comparison of L1 and L3 conformations of the VEGFR-1 ligands PlGF (cyan), VEGF-A (magenta), and VEGF-B (orange) in complex with the VEGFR-1 D2–3 homology model. A homology model of B-L1^P suggests a PlGF/VEGF-A–like L1 conformation stabilized by the conserved ionic interactions Glu^{46}-Arg^{56} and Tyr^{46}-Ser^{94} (PlGF/VEGF-B numbering). (**E**) Schematic model of differential VEGFR-1 binding by PlGF and VEGF-B. Unlike VEGF-B, PlGF (or B-L1^P) interaction with VEGFR-1 can lead to an "activating" mode of VEGFR-1 dimer conformation with RTK domains brought close enough together to initiate receptor phosphorylation and downstream signaling.

DISCUSSION

Here, we provide new data that help in understanding why two specific ligands of VEGFR-1 with similar overall structures display marked differences in their biological activities. We show that the differential VEGFR-1 binding and activation involving ligand L1 interactions with receptor D3 explain the differences in the biological activities, and are thus critical for VEGFR activation. Furthermore, we show that swapping the PlGF-derived L1 to VEGF-B confers the chimeric ligand the ability to activate VEGFR-2, downstream signaling, and angiogenic responses.

In general, RTKs are activated by growth factor–induced dimerization, and the bivalent VEGFs induce VEGFR cross-linking through the ligand-binding domains D2–3 (*35*). VEGFR ligand binding is followed by homotypic interactions in the membrane-proximal domains D4–5 and D7, which are crucial for receptor activation (*36*–*38*). We and others have shown that targeting such homotypic interactions with blocking antibodies that do not affect ligand binding can inhibit VEGFR activation (*39*–*41*).

The extracellular domains of VEGFRs show interdomain flexibility, including the D2–3 junction that forms the binding site for the ligand. A full ligand-binding domain (D2–3) structure has been described for VEGFR-2 complexes with VEGF-A, VEGF-C, and VEGF-E (*28*, *42*). There are notable differences in the D2–3 twist angles of the receptor monomers (6° to 25°) around the twofold symmetry axis of the homodimeric ligands. The complexes have similar D2 binding modes; their differences consist of variation in D2–3 interdomain angles due to different ligand interactions with D3 and variation in the crystal packing. VEGF-A induces strong VEGFR-2 activation. The

~1000-fold loss of binding affinity caused by D3 deletion (*26*) indicates the importance of D3 interactions and D3 orientation in priming the subsequent homotypic interactions and signal transduction.

The VEGFR family of type V RTKs is closely related to the type III RTKs consisting of a diverse family of receptors characterized by five extracellular Ig-like domains, in which ligand binding is also centered between D2 and D3. The ligands of type III RTKs use either the cystine-knot-β-sheet fold (as for the type V RTKs) or the four-helix-bundle fold (*43*–*45*). The dimerization and activation of the prototypic KIT receptor by its ligand involves reorientation of the Ig-like domains D4 and D5 to allow interaction across the dimer interface (*46*). Structural studies on colony-stimulating factor 1 receptor (CSF-1R) revealed a large reconfiguration of the D2–3 elbow between the binding of its ligands CSF-1 and IL-34 (*47*). CSF-1 and IL-34 induce differential signaling (*48*), suggesting that the reorientation of the CSF-1R domains may modulate its signaling potency. Also, the D2–3 junction in the two platelet-derived growth factor receptors (PDGFRs) appears to be flexible until the ligand binds (*49*). Similarly to VEGFRs, the results with type III RTKs thus emphasize the importance of the spatial reorientation of both the ligand-binding (D2–3) and the membrane-proximal domains.

Deletion of D3 from VEGFR-1 D1–3 results in about 20- and 500-fold decreased VEGF-A and PlGF binding affinities, respectively (*24*, *26*). Our experiments on D3 dependence of VEGF-B and PlGF binding to VEGFR-1 confirmed the importance of D3 interactions for the high-affinity binding of PlGF. Also, consistent with the about 10-fold increased affinity, PlGF binding to D1–3 was accompanied with an about 2-fold larger enthalpy change than binding to D1–2. Instead, VEGF-B bound to both receptor fragments with similar affinity, and the thermodynamic profiles were more similar, suggesting that D2 determines VEGF-B binding and, compared to PlGF, VEGF-B has either fewer or different interactions with D3. This may reflect differences in ligand-induced D2–3 reorientation and VEGFR-1 dimerization.

Comparison of the VEGF-B/PlGF loop swaps to the parental growth factors in VEGFR-1 binding, activation, and angiogenesis assays indicated that the L3 swaps had only moderate effects on VEGFR-1 activation, whereas the L1 swaps revealed strong gain-of-function (B-L1^{P}) and loss-of-function (P-L1^{B}) effects both in VEGFR-1 stimulation in vitro and in the angiogenesis assays in mouse skeletal muscle. In the cellular assay, native VEGF-B was a poor activator of VEGFR-1, suggesting less productive VEGFR-1 dimerization. The importance of L1 for VEGFR-1 activation was further confirmed by loop swaps between VEGF-A and VEGF-B, in which A-L1^{B} lost its VEGFR-1–stimulating activity but retained VEGFR-1 binding, and B-L1^{A} behaved similarly to B-L1^{P}. Consistent with the sequence and structural similarity, the L1 swaps between VEGF-A and PlGF did not alter receptor specificities. B-L1^{P} and PlGF also increased the vascularity of skeletal muscle, unlike P-L1^{B} or VEGF-B. Thus, although the angiogenic activity likely involves cross talk with VEGFR-2, differences between VEGF-B and PlGF in VEGFR-1 binding and activation are mainly determined by L1.

The strong D3 dependence of VEGFR-1 binding and the importance of PlGF L1 in VEGFR-1 activation suggest the existence of specific interactions between PlGF L1 and VEGFR-1 D3. Consistent with the favorable enthalpy observed in PlGF binding, several charged residues (Arg^{280}-Asp^{283}) located in VEGFR-1 D3 are important for PlGF binding (*25*). Comparison of the VEGFR-1 D3 homology model and the PlGF/VEGFR-1 D2 complex structure to the ligand/VEGFR-2 D2–3 complex structures (*28*, *42*) indicates close proximity between VEGFR-1 Arg^{280}-Asp^{283} and PlGF L1, although detailed interactions remain to be elucidated. Our data indicate that B-L1^{P} may adopt the parental L1 conformation, interactions with D3, and the mode of VEGFR-1 activation. On the other hand, the P-L1^{B} and VEGF-B data suggest that VEGF-B L1 is likely to have different, if any, interactions with D3 that do not support VEGFR-1 activation. PDGF-B, which is a cystine-knot ligand similar to VEGFs, also has major determinants of PDGFRβ D3 binding and receptor activation in L1 (*49*).

The other interesting finding in our study was the low-affinity VEGFR-2 binding and activation by B-L1^{P}. This gain-of-function activity of B-L1^{P} appeared as a result of the L1 swap between the two ligands, which by themselves are not able to bind to or directly activate VEGFR-2. The B-L1^{A} swap resulted in a similar gain of VEGFR-2–stimulating activity. Considering the similarity in the topology of the VEGF family members and in the PlGF and VEGF-A L1 amino acid sequences (53%; fig. S1, A and B), PlGF and VEGF-A L1 could confer some VEGF-A properties, such as VEGFR-2 binding and activation, on their VEGF-B derivatives. Although this activity of B-L1^{P} was weaker than that of VEGF-A, we showed that B-L1^{P} promotes VEGFR-2 tyrosine phosphorylation as well as downstream signaling in vitro and in vivo. On the other hand, PlGF participates in VEGFR-2 phosphorylation and activation through the formation of PlGF/VEGF-A heterodimers, which can bind to and activate VEGFR-1/VEGFR-2 heterodimers (*50*–*52*). This indicates that some receptor-binding epitopes in PlGF (L1 and L3 or L2 and αN in the opposite poles) are compatible with VEGFR-2 binding because PlGF and VEGF-A subunits contribute to both of the receptor-binding interfaces of the heterodimer. Our data suggest that PlGF L1 in B-L1^{P} and VEGF-A L1 in B-L1^{A} could adopt similar VEGFR-2 D3 interactions as VEGF-A.

In conclusion, we demonstrate here that differences in VEGFR-1–mediated biological activities between VEGF-B and PlGF are mainly determined by L1, which interacts with D3 of VEGFRs. PlGF L1 interactions with D3 of VEGFR-1 seem to explain the ability of PlGF to activate VEGFR-1. The high-affinity binding of VEGF-B to D2 of VEGFR-1 and the lack of PlGF-like L1-D3 interactions may provide inadequate priming of its membrane-proximal domains for homotypic interactions necessary for VEGFR activation. This mode of binding does not activate the receptor (Fig. 5E). Instead, VEGF-B may prevent the other ligands, such as VEGF-A, from interacting with the occupied VEGFR-1, thus redirecting VEGF-A signaling through VEGFR-2, as previously proposed for PlGF (*53*). This scenario would apply to organs with abundant endogenous VEGF-B protein, such as the embryonic heart, where VEGF-B may act as a strong modulator of the main angiogenic factor VEGF-A. On the other hand, maximal VEGF-B activity would be dependent on the available endogenous VEGF-A for VEGFR-2 activation. Thus, unlike for VEGF-A and PlGF, administration of even high concentrations of VEGF-B would not lead to harmful consequences, such as vascular leakage or hemangioma formation, that hindered the development of proangiogenic therapies with VEGF-A (*54*, *55*).

MATERIALS AND METHODS

Antibodies

The following antibodies were used in the study: rabbit anti–phospho-VEGFR-2 (Tyr^{1175}) (Cell Signaling, cat. #2478) and anti–phospho-VEGFR-1 (Tyr^{1213}) (R&D Systems, cat. #AF4170); goat anti-mouse VEGFR-2 (R&D Systems, cat. #AF644); mouse anti-pY (clone 4G10) (Millipore, cat. #05-321) and rabbit anti–VEGFR-1 (Santa Cruz Biotechnology, cat. #sc-316) and anti–VEGFR-2 (Santa Cruz Biotechnology, cat. #sc-504); rabbit anti–phospho-p44/42 MAPK (T202/Y204) and anti–p44/42 MAPK (Cell Signaling, cat. #9101 and 9102); rabbit anti–phospho-Akt (S473) and rabbit anti-Akt (Cell Signaling, cat. #9271 and 9272); mouse anti–Penta-His (Qiagen, cat. #34660); rat anti-mouse CD31 (PECAM-1) (BD Biosciences, cat. #553370); and mouse anti–SMA-Cy3 (Sigma, cat.

#C 6198). Secondary species-specific Alexa-conjugated antibodies were from Invitrogen.

Cloning

AAV vectors (psubCMV-WPRE or psubCAG-WPRE) encoding mouse VEGF-B186, mouse PlGF, and human serum albumin were described in our previous publication (*9*). B-L1^{P} and P-L1^{B} replacement constructs were cloned into the psubCAG-WPRE vector in a similar way. Truncated mouse VEGF-B and PlGF, containing sequences encoded by exons 1 to 5, as well as B-L1^{P}, P-L1^{B}, A-L1^{P}, P-L1^{A}, and B-L1^{A} replacement chimeras, were cloned into the pFastBac1 vector (Invitrogen) for protein production in Sf21 insect cells.

Protein production and purification

Mouse PlGF (residues 19 to 137, encoded by exons 1 to 5), VEGF-B (residues 23 to 36, encoded by exons 1 to 5), human VEGF-A (residues 27 to 191), and their L1 (residues 56 to 70, 55 to 69, and 61 to 74, respectively) swaps were produced with a C-terminal His-tag in Sf21 insect cells using the baculovirus system. VEGF-B, B-L1^{P}, and B-L1^{A} contain a Q96N/R98T double mutation to create an N-glycosylation site similar to that in PlGF. The proteins were purified by Ni^{2+}-charged chelating Sepharose (GE Healthcare) followed by gel filtration on a Superdex 200 (GE Healthcare) column. VEGF-C was produced and purified similarly (*28*). Human VEGFR-1 domains 1 to 2 (VEGFR-1 D1–2, residues 23 to 224) and domains 1 to 3 (VEGFR-1 D1–3, residues 23 to 331) and human VEGFR-2 domains 2 to 3 (VEGFR-2 D2–3, residues 118 to 326) were produced with a C-terminal Factor Xa cleavage site and an Fc-tag (IgG1) using the baculovirus system. The proteins were purified by protein A–Sepharose (GE Healthcare) followed by gel filtration on the Superdex 200 column or by buffer exchange using Fast Desalting Column (HR 10/10, GE Healthcare). Monomeric VEGFR-1 D1–2 and D1–3 constructs were prepared by Fc-tag removal using Factor Xa (GE Healthcare).

Production of rAAV serotype 9

rAAVs (serotype 9) encoding mouse VEGF-B186, PlGF, and the replacement chimeras B-L1^{P} and P-L1^{B} were produced and purified by a three-plasmid transfection method, as previously described (*56*).

Analysis of growth factor expression and activity

Growth factor–containing supernatants were produced by rAAV vector transfection of 293T cells metabolically labeled with [^{35}S]Cys/Met (Amersham Biosciences and GE Healthcare). The growth factors were precipitated with VEGFR-1–Ig and protein A–Sepharose, followed by analysis by gel electrophoresis and autoradiography. The hVEGFR-1/EpoR-BaF3 cell line used for the ligand activity assay is a previously described derivative of the IL-3–dependent mouse pro-B cell line BaF3 (*31*). The MTT cell proliferation assay was performed essentially as described (*56*).

Analysis of VEGFR-2 phosphorylation and VEGFR-1/VEGFR-2 heterodimerization in cultured endothelial cells

BECs or HUVECs (PromoCell) were used as indicated. The PAE cell line was obtained from L. Claesson-Welsh (Uppsala, Sweden). NIH 3T3 cells (American Type Culture Collection) were transfected with a retrovirus vector encoding human VEGFR-2. The cells were starved overnight and then stimulated for 5 or 10 min with the ligands, as indicated. VEGF-A was used at 100 ng/ml (Fig. 4, A, B, and C) or 50 ng/ml (Fig. 4, E and G); all the other proteins were used at 500 ng/ml (Fig. 4, A, B, E, and G) or 1 μg/ml (Fig. 4C). In some instances, varying concentrations of B-L1^{P} were used, ranging from 50 to 500 ng/ml, as indicated in Fig. 4E, and for the experiment shown in Fig. 4G, VEGF-B was used at 20 μg/ml. After growth factor treatment, the cells were lysed in lysis buffer [phosphate-buffered saline (PBS), containing 0.5% Triton X-100, 0.5% NP-40, and protease plus phosphatase inhibitors]. The lysates were subjected to gel electrophoresis either immediately or after the immunoprecipitation step as indicated, transferred onto a polyvinylidene difluoride membrane, and Western-blotted with the indicated antibodies.

Binding assays

Thermodynamic characterization of VEGF-B and PlGF binding to the monomeric VEGFR-1 deletion mutants VEGFR-1 D1–2 and VEGFR-1 D1–3 was carried out at +27 using a VP-ITC calorimeter (MicroCal) as described (*28*). B-L1^{P} binding to VEGFR-1 D1–3 and to the Fc-tagged VEGFR-2 D2–3 was analyzed similarly. The data were processed using MicroCal Origin 7.0 software. The relative binding affinities to the Fc-tagged VEGFR-2 D2–3 were analyzed by an enzyme-linked immunoassay. VEGFR-2 binding to VEGF-A was competed by VEGF-B, PlGF, B-L1^{P}, and VEGF-C, and the IC_{50} values were determined using a one-site binding model and nonlinear regression analysis in Prism v3.02 (GraphPad Software).

Expression and activity analysis of VEGFR-1 ligands in mouse skeletal muscle

Twelve-week-old female FVB/N mice were anesthetized with xylazine (Rompun vet, Bayer Healthcare) and ketamine (Ketalar, Pfizer), and a dose of 3×10^{10} rAAV particles (in 30-μl volume) was injected into each tibialis anterior muscle. All mouse experiments were approved by the Provincial State Office of Southern Finland and carried out in accordance with the institutional guidelines. After 2 weeks, the tibialis anterior muscles were isolated, embedded in optimum cutting temperature compound (Tissue-Tek), sectioned, acetone-fixed, and immunostained with the indicated antibodies. The microvessel area density was quantified using ImageJ software (National Institutes of Health).

Analysis of protein phosphorylation in vivo

Pure growth factors (in 100 μl of PBS) were injected at a dose of 20 μg per mouse or at doses indicated in Fig. 3C to anesthetized 10- to 12-week-old FVB/NJ mice. After 10 min, unless otherwise indicated, the tissues were isolated and flash-frozen in liquid nitrogen until use. For analysis of phosphorylated and total VEGFR-1 or VEGFR-2, the tissues were thawed and homogenized in ice-cold lysis buffer. Tissue lysates (150 μg of total soluble protein) were subjected to Western blotting or immunoprecipitation followed by Western blotting (for phospho-VEGFR-1 Tyr^{1213} determination).

Homology modeling

A VEGFR-1 D2–3 homology model for residues 134 to 333 of mouse VEGFR-1 was prepared using crystal structures of VEGFR-1 D2 (PDB code 1FLT) and VEGFR-2 D3 (PDB code 2X1X) as templates in Swiss-Model. Similarly, B-L1^{P} was modeled using PlGF (PDB code 1RV6) as a template. To obtain the 2:2 models, the VEGFR-1 D2–3 model, the three ligands—PlGF, VEGF-A, and VEGF-B—from the VEGFR-1 D2 complex structures (PDB codes 1FLT, 1RV6, and 2AXC, respectively), and the B-L1^{P} model were superimposed with the corresponding chains in the VEGF-A/VEGFR-2 D2–3 complex (PDB code 3V2A) in Coot (*57*).

Statistical analysis

If equal variances were assumed, we evaluated statistical significance by one-way analysis of variance (ANOVA), followed by the Dunnett (two-sided) post hoc test, with $P < 0.05$ regarded as significant. Where pairwise comparisons between experimental groups were made, the Tukey test was used. If the variances were not equal, the Games-Howell test was used as a

post hoc test, with $P < 0.05$ regarded as significant. The results are presented as means ± SD.

SUPPLEMENTARY MATERIALS

www.sciencesignaling.org/cgi/content/full/6/282/ra52/DC1

Fig. S1. Comparison of the amino acid sequences of VEGFR-1 ligand loops.

Fig. S2. Replacement of VEGF-A L1 with the VEGF-B–derived L1 does not affect VEGFR-1 binding, but inhibits VEGFR-1 activation.

Fig. S3. Pretreatment of PAE–VEGFR-2 cells with high molar excess of VEGF-B does not reduce the VEGFR-2 phosphorylation induced by B-L1^P or VEGF-A.

Fig. S4. Analysis of L1 swap chimeras between VEGF-A and PlGF.

REFERENCES AND NOTES

1. A. S. Chung, N. Ferrara, Developmental and pathological angiogenesis. *Annu. Rev. Cell Dev. Biol.* **27**, 563–584 (2011).
2. S. Koch, S. Tugues, X. Li, L. Gualandi, L. Claesson-Welsh, Signal transduction by vascular endothelial growth factor receptors. *Biochem. J.* **437**, 169–183 (2011).
3. M. Shibuya, L. Claesson-Welsh, Signal transduction by VEGF receptors in regulation of angiogenesis and lymphangiogenesis. *Exp. Cell Res.* **312**, 549–560 (2006).
4. D. I. Holmes, I. Zachary, The vascular endothelial growth factor (VEGF) family: Angiogenic factors in health and disease. *Genome Biol.* **6**, 209 (2005).
5. S. De Falco, The discovery of placenta growth factor and its biological activity. *Exp. Mol. Med.* **44**, 1–9 (2012).
6. M. Dewerchin, P. Carmeliet, PlGF: A multitasking cytokine with disease-restricted activity. *Cold Spring Harb. Perspect. Med.* **2**, a011056 (2012).
7. Y. Cao, Positive and negative modulation of angiogenesis by VEGFR1 ligands. *Sci. Signal.* **2**, re1 (2009).
8. B. Olofsson, K. Pajusola, A. Kaipainen, G. von Euler, V. Joukov, O. Saksela, A. Orpana, R. F. Pettersson, K. Alitalo, U. Eriksson, Vascular endothelial growth factor B, a novel growth factor for endothelial cells. *Proc. Natl. Acad. Sci. U.S.A.* **93**, 2576–2581 (1996).
9. M. Bry, R. Kivelä, T. Holopainen, A. Anisimov, T. Tammela, J. Soronen, J. Silvola, A. Saraste, M. Jeltsch, P. Korpisalo, P. Carmeliet, K. B. Lemström, M. Shibuya, S. Ylä-Herttuala, L. Alhonen, E. Mervaala, L. C. Andersson, J. Knuuti, K. Alitalo, Vascular endothelial growth factor-B acts as a coronary growth factor in transgenic rats without inducing angiogenesis, vascular leak, or inflammation. *Circulation* **122**, 1725–1733 (2010).
10. J. E. Lähteenvuo, M. T. Lähteenvuo, A. Kivelä, C. Rosenlew, A. Falkevall, J. Klar, T. Heikura, T. T. Rissanen, E. Vähäkangas, P. Korpisalo, B. Enholm, P. Carmeliet, K. Alitalo, U. Eriksson, S. Ylä-Herttuala, Vascular endothelial growth factor-B induces myocardium-specific angiogenesis and arteriogenesis via vascular endothelial growth factor receptor-1– and neuropilin receptor-1–dependent mechanisms. *Circulation* **119**, 845–856 (2009).
11. R. J. Levine, S. E. Maynard, C. Qian, K. H. Lim, L. J. England, K. F. Yu, E. F. Schisterman, R. Thadhani, B. P. Sachs, F. H. Epstein, B. M. Sibai, V. P. Sukhatme, S. A. Karumanchi, Circulating angiogenic factors and the risk of preeclampsia. *N. Engl. J. Med.* **350**, 672–683 (2004).
12. S. E. Maynard, J. Y. Min, J. Merchan, K. H. Lim, J. Li, S. Mondal, T. A. Libermann, J. P. Morgan, F. W. Sellke, I. E. Stillman, F. H. Epstein, V. P. Sukhatme, S. A. Karumanchi, Excess placental soluble fms-like tyrosine kinase 1 (sFlt1) may contribute to endothelial dysfunction, hypertension, and proteinuria in preeclampsia. *J. Clin. Invest.* **111**, 649–658 (2003).
13. K. Aase, G. von Euler, X. Li, A. Pontén, P. Thorén, R. Cao, Y. Cao, B. Olofsson, S. Gebre-Medhin, M. Pekny, K. Alitalo, C. Betsholtz, U. Eriksson, Vascular endothelial growth factor-B–deficient mice display an atrial conduction defect. *Circulation* **104**, 358–364 (2001).
14. D. Bellomo, J. P. Headrick, G. U. Silins, C. A. Paterson, P. S. Thomas, M. Gartside, A. Mould, M. M. Cahill, I. D. Tonks, S. M. Grimmond, S. Townson, C. Wells, M. Little, M. C. Cummings, N. K. Hayward, G. F. Kay, Mice lacking the vascular endothelial growth factor-B gene (*Vegfb*) have smaller hearts, dysfunctional coronary vasculature, and impaired recovery from cardiac ischemia. *Circ. Res.* **86**, E29–E35 (2000).
15. P. Carmeliet, L. Moons, A. Luttun, V. Vincenti, V. Compernolle, M. De Mol, Y. Wu, F. Bono, L. Devy, H. Beck, D. Scholz, T. Acker, T. DiPalma, M. Dewerchin, A. Noel, I. Stalmans, A. Barra, S. Blacher, T. VandenDriessche, A. Ponten, U. Eriksson, K. H. Plate, J. M. Foidart, W. Schaper, D. S. Charnock-Jones, D. J. Hicklin, J. M. Herbert, D. Collen, M. G. Persico, Synergism between vascular endothelial growth factor and placental growth factor contributes to angiogenesis and plasma extravasation in pathological conditions. *Nat. Med.* **7**, 575–583 (2001).
16. S. Hiratsuka, Y. Maru, A. Okada, M. Seiki, T. Noda, M. Shibuya, Involvement of Flt-1 tyrosine kinase (vascular endothelial growth factor receptor-1) in pathological angiogenesis. *Cancer Res.* **61**, 1207–1213 (2001).
17. C. Fischer, B. Jonckx, M. Mazzone, S. Zacchigna, S. Loges, L. Pattarini, E. Chorianopoulos, L. Liesenborghs, M. Koch, M. De Mol, M. Autiero, S. Wyns, S. Plaisance, L. Moons, N. van Rooijen, M. Giacca, J. M. Stassen, M. Dewerchin, D. Collen, P. Carmeliet, Anti-PlGF inhibits growth of VEGF(R)-inhibitor-resistant tumors without affecting healthy vessels. *Cell* **131**, 463–475 (2007).
18. S. Van de Veire, I. Stalmans, F. Heindryckx, H. Oura, A. Tijeras-Raballand, T. Schmidt, S. Loges, I. Albrecht, B. Jonckx, S. Vinckier, C. Van Steenkiste, S. Tugues, C. Rolny, M. De Mol, D. Dettori, P. Hainaud, L. Coenegrachts, J. O. Contreres, T. Van Bergen, H. Cuervo, W. H. Xiao, C. Le Henaff, I. Buysschaert, B. Kharabi Masouleh, A. Geerts, T. Schomber, P. Bonnin, V. Lambert, J. Haustraete, S. Zacchigna, J. M. Rakic, W. Jiménez, A. Noél, M. Giacca, I. Colle, J. M. Foidart, G. Tobelem, M. Morales-Ruiz, J. Vilar, P. Maxwell, S. A. Vinores, G. Carmeliet, M. Dewerchin, L. Claesson-Welsh, E. Dupuy, H. Van Vlierberghe, G. Christofori, M. Mazzone, M. Detmar, D. Collen, P. Carmeliet, Further pharmacological and genetic evidence for the efficacy of PlGF inhibition in cancer and eye disease. *Cell* **141**, 178–190 (2010).
19. C. Bais, X. Wu, J. Yao, S. Yang, Y. Crawford, K. McCutcheon, C. Tan, G. Kolumam, J. M. Vernes, J. Eastham-Anderson, P. Haughney, M. Kowanetz, T. Hagenbeek, I. Kasman, H. B. Reslan, J. Ross, N. Van Bruggen, R. A. Carano, Y. J. Meng, J. A. Hongo, J. P. Stephan, M. Shibuya, N. Ferrara, PlGF blockade does not inhibit angiogenesis during primary tumor growth. *Cell* **141**, 166–177 (2010).
20. J. Yao, X. Wu, G. Zhuang, I. M. Kasman, T. Vogt, V. Phan, M. Shibuya, N. Ferrara, C. Bais, Expression of a functional VEGFR-1 in tumor cells is a major determinant of anti-PlGF antibodies efficacy. *Proc. Natl. Acad. Sci. U.S.A.* **108**, 11590–11595 (2011).
21. I. Albrecht, L. Kopfstein, K. Strittmatter, T. Schomber, A. Falkevall, C. E. Hagberg, P. Lorentz, M. Jeltsch, K. Alitalo, U. Eriksson, G. Christofori, K. Pietras, Suppressive effects of vascular endothelial growth factor-B on tumor growth in a mouse model of pancreatic neuroendocrine tumorigenesis. *PLoS One* **5**, e14109 (2010).
22. T. Davis-Smyth, H. Chen, J. Park, L. G. Presta, N. Ferrara, The second immunoglobulin-like domain of the VEGF tyrosine kinase receptor Flt-1 determines ligand binding and may initiate a signal transduction cascade. *EMBO J.* **15**, 4919–4927 (1996).
23. H. W. Christinger, G. Fuh, A. M. de Vos, C. Wiesmann, The crystal structure of placental growth factor in complex with domain 2 of vascular endothelial growth factor receptor-1. *J. Biol. Chem.* **279**, 10382–10388 (2004).
24. C. Wiesmann, G. Fuh, H. W. Christinger, C. Eigenbrot, J. A. Wells, A. M. de Vos, Crystal structure at 1.7 Å resolution of VEGF in complex with domain 2 of the Flt-1 receptor. *Cell* **91**, 695–704 (1997).
25. T. Davis-Smyth, L. G. Presta, N. Ferrara, Mapping the charged residues in the second immunoglobulin-like domain of the vascular endothelial growth factor/placenta growth factor receptor Flt-1 required for binding and structural stability. *J. Biol. Chem.* **273**, 3216–3222 (1998).
26. G. Fuh, B. Li, C. Crowley, B. Cunningham, J. A. Wells, Requirements for binding and signaling of the kinase domain receptor for vascular endothelial growth factor. *J. Biol. Chem.* **273**, 11197–11204 (1998).
27. S. Iyer, P. I. Darley, K. R. Acharya, Structural insights into the binding of vascular endothelial growth factor-B by VEGFR-1$_{D2}$: Recognition and specificity. *J. Biol. Chem.* **285**, 23779–23789 (2010).
28. V. M. Leppänen, A. E. Prota, M. Jeltsch, A. Anisimov, N. Kalkkinen, T. Strandin, H. Lankinen, A. Goldman, K. Ballmer-Hofer, K. Alitalo, Structural determinants of growth factor binding and specificity by VEGF receptor 2. *Proc. Natl. Acad. Sci. U.S.A.* **107**, 2425–2430 (2010).
29. A. Kiba, N. Yabana, M. Shibuya, A set of loop-1 and -3 structures in the novel vascular endothelial growth factor (VEGF) family member, VEGF-E$_{NZ-7}$, is essential for the activation of VEGFR-2 signaling. *J. Biol. Chem.* **278**, 13453–13461 (2003).
30. M. G. Achen, S. Roufail, T. Domagala, B. Catimel, E. C. Nice, D. M. Geleick, R. Murphy, A. M. Scott, C. Caesar, T. Makinen, K. Alitalo, S. A. Stacker, Monoclonal antibodies to vascular endothelial growth factor-D block its interactions with both VEGF receptor-2 and VEGF receptor-3. *Eur. J. Biochem.* **267**, 2505–2515 (2000).
31. T. Mäkinen, T. Veikkola, S. Mustjoki, T. Karpanen, B. Catimel, E. C. Nice, L. Wise, A. Mercer, H. Kowalski, D. Kerjaschki, S. A. Stacker, M. G. Achen, K. Alitalo, Isolated lymphatic endothelial cells transduce growth, survival and migratory signals via the VEGF-C/D receptor VEGFR-3. *EMBO J.* **20**, 4762–4773 (2001).
32. E. Landgren, P. Schiller, Y. Cao, L. Claesson-Welsh, Placenta growth factor stimulates MAP kinase and mitogenicity but not phospholipase C-γ and migration of endothelial cells expressing Flt 1. *Oncogene* **16**, 359–367 (1998).
33. M. J. Cudmore, P. W. Hewett, S. Ahmad, K. Q. Wang, M. Cai, B. Al-Ani, T. Fujisawa, B. Ma, S. Sissaoui, W. Ramma, M. R. Miller, D. E. Newby, Y. Gu, B. Barleon, H. Weich, A. Ahmed, The role of heterodimerization between VEGFR-1 and VEGFR-2 in the regulation of endothelial cell homeostasis. *Nat. Commun.* **3**, 972 (2012).
34. K. Huang, C. Andersson, G. M. Roomans, N. Ito, L. Claesson-Welsh, Signaling properties of VEGF receptor-1 and -2 homo- and heterodimers. *Int. J. Biochem. Cell Biol.* **33**, 315–324 (2001).
35. M. A. Lemmon, J. Schlessinger, Cell signaling by receptor tyrosine kinases. *Cell* **141**, 1117–1134 (2010).
36. K. Kisko, M. S. Brozzo, J. Missimer, T. Schleier, A. Menzel, V. M. Leppänen, K. Alitalo, T. Walzthoeni, R. Aebersold, K. Ballmer-Hofer, Structural analysis of vascular endothelial growth factor receptor-2/ligand complexes by small-angle X-ray solution scattering. *FASEB J.* **25**, 2980–2986 (2011).

37. C. Ruch, G. Skiniotis, M. O. Steinmetz, T. Walz, K. Ballmer-Hofer, Structure of a VEGF-VEGF receptor complex determined by electron microscopy. *Nat. Struct. Mol. Biol.* **14**, 249–250 (2007).
38. Y. Yang, P. Xie, Y. Opatowsky, J. Schlessinger, Direct contacts between extracellular membrane-proximal domains are required for VEGF receptor activation and cell signaling. *Proc. Natl. Acad. Sci. U.S.A.* **107**, 1906–1911 (2010).
39. C. A. Hyde, A. Giese, E. Stuttfeld, J. Abram Saliba, D. Villemagne, T. Schleier, H. K. Binz, K. Ballmer-Hofer, Targeting extracellular domains D4 and D7 of vascular endothelial growth factor receptor 2 reveals allosteric receptor regulatory sites. *Mol. Cell. Biol.* **32**, 3802–3813 (2012).
40. J. Kendrew, C. Eberlein, B. Hedberg, K. McDaid, N. R. Smith, H. M. Weir, S. R. Wedge, D. C. Blakey, I. Foltz, J. Zhou, J. S. Kang, S. T. Barry, An antibody targeted to VEGFR-2 Ig domains 4-7 inhibits VEGFR-2 activation and VEGFR-2–dependent angiogenesis without affecting ligand binding. *Mol. Cancer Ther.* **10**, 770–783 (2011).
41. D. Tvorogov, A. Anisimov, W. Zheng, V. M. Leppänen, T. Tammela, S. Laurinavicius, W. Holnthoner, H. Heloterä, T. Holopainen, M. Jeltsch, N. Kalkkinen, H. Lankinen, P. M. Ojala, K. Alitalo, Effective suppression of vascular network formation by combination of antibodies blocking VEGFR ligand binding and receptor dimerization. *Cancer Cell* **18**, 630–640 (2010).
42. M. S. Brozzo, S. Bjelić, K. Kisko, T. Schleier, V. M. Leppänen, K. Alitalo, F. K. Winkler, K. Ballmer-Hofer, Thermodynamic and structural description of allosterically regulated VEGFR-2 dimerization. *Blood* **119**, 1781–1788 (2012).
43. C. H. Heldin, B. Westermark, Mechanism of action and in vivo role of platelet-derived growth factor. *Physiol. Rev.* **79**, 1283–1316 (1999).
44. D. Metcalf, Hematopoietic cytokines. *Blood* **111**, 485–491 (2008).
45. S. N. Savvides, T. Boone, P. Andrew Karplus, Flt3 ligand structure and unexpected commonalities of helical bundles and cystine knots. *Nat. Struct. Biol.* **7**, 486–491 (2000).
46. S. Yuzawa, Y. Opatowsky, Z. Zhang, V. Mandiyan, I. Lax, J. Schlessinger, Structural basis for activation of the receptor tyrosine kinase KIT by stem cell factor. *Cell* **130**, 323–334 (2007).
47. X. Ma, W. Y. Lin, Y. Chen, S. Stawicki, K. Mukhyala, Y. Wu, F. Martin, J. F. Bazan, M. A. Starovasnik, Structural basis for the dual recognition of helical cytokines IL-34 and CSF-1 by CSF-1R. *Structure* **20**, 676–687 (2012).
48. T. Chihara, S. Suzu, R. Hassan, N. Chutiwitoonchai, M. Hiyoshi, K. Motoyoshi, F. Kimura, S. Okada, IL-34 and M-CSF share the receptor Fms but are not identical in biological activity and signal activation. *Cell Death Differ.* **17**, 1917–1927 (2010).
49. A. H. Shim, H. Liu, P. J. Focia, X. Chen, P. C. Lin, X. He, Structures of a platelet-derived growth factor/propeptide complex and a platelet-derived growth factor/receptor complex. *Proc. Natl. Acad. Sci. U.S.A.* **107**, 11307–11312 (2010).
50. M. Autiero, J. Waltenberger, D. Communi, A. Kranz, L. Moons, D. Lambrechts, J. Kroll, S. Plaisance, M. De Mol, F. Bono, S. Kliche, G. Fellbrich, K. Ballmer-Hofer, D. Maglione, U. Mayr-Beyrle, M. Dewerchin, S. Dombrowski, D. Stanimirovic, P. Van Hummelen, C. Dehio, D. J. Hicklin, G. Persico, J. M. Herbert, D. Communi, M. Shibuya, D. Collen, E. M. Conway, P. Carmeliet, Role of PlGF in the intra- and intermolecular cross talk between the VEGF receptors Flt1 and Flk1. *Nat. Med.* **9**, 936–943 (2003).
51. J. DiSalvo, M. L. Bayne, G. Conn, P. W. Kwok, P. G. Trivedi, D. D. Soderman, T. M. Palisi, K. A. Sullivan, K. A. Thomas, Purification and characterization of a naturally occurring vascular endothelial growth factor×placenta growth factor heterodimer. *J. Biol. Chem.* **270**, 7717–7723 (1995).
52. V. Tarallo, L. Vesci, O. Capasso, M. T. Esposito, T. Riccioni, L. Pastore, A. Orlandi, C. Pisano, S. De Falco, A placental growth factor variant unable to recognize vascular endothelial growth factor (VEGF) receptor-1 inhibits VEGF-dependent tumor angiogenesis via heterodimerization. *Cancer Res.* **70**, 1804–1813 (2010).
53. C. Fischer, M. Mazzone, B. Jonckx, P. Carmeliet, FLT1 and its ligands VEGFB and PlGF: Drug targets for anti-angiogenic therapy? *Nat. Rev. Cancer* **8**, 942–956 (2008).
54. M. Hedman, J. Hartikainen, S. Ylä-Herttuala, Progress and prospects: Hurdles to cardiovascular gene therapy clinical trials. *Gene Ther.* **18**, 743–749 (2011).
55. S. Reginato, R. Gianni-Barrera, A. Banfi, Taming of the wild vessel: Promoting vessel stabilization for safe therapeutic angiogenesis. *Biochem. Soc. Trans.* **39**, 1654–1658 (2011).
56. A. Anisimov, A. Alitalo, P. Korpisalo, J. Soronen, S. Kaijalainen, V. M. Leppänen, M. Jeltsch, S. Ylä-Herttuala, K. Alitalo, Activated forms of VEGF-C and VEGF-D provide improved vascular function in skeletal muscle. *Circ. Res.* **104**, 1302–1312 (2009).
57. P. Emsley, K. Cowtan, Coot: Model-building tools for molecular graphics. *Acta Crystallogr. D Biol. Crystallogr.* **60**, 2126–2132 (2004).

Acknowledgments: We thank L. Claesson-Welsh for providing the PAE cell line; M. Bry for useful comments on the manuscript; J. Soronen for help in the beginning of the project; T. Tainola, T. Laakkonen, and J. Koponen for expert technical assistance; the rAAV Gene Transfer and Cell Therapy Core Facility of Biocentrum Finland for vector production; the Biomedicum Imaging Unit for microscope support; and the staff at the Biomedicum Helsinki and the Haartman Institute Animal Facilities for excellent animal husbandry. **Funding:** This study was supported by the Academy of Finland (262976), European Research Council (TX-FACTORS, grant number ERC-2010-AdG-268804), the Sigrid Juselius Foundation, the Finnish Foundation for Cardiovascular Research, Leducq Foundation, and Biocenter Finland. G.Z. was supported by personal grants from the Finnish Medical Foundation, the K. Albin Johansson Foundation, the Maud Kuistila Foundation, and the Oskar Öflund Foundation. **Author contributions:** A.A. and V.-M.L. performed the research, analyzed the data, and wrote the paper. D.T., G.Z., M.J., T.H., and S.K. performed the research. K.A. designed the research and wrote the paper. **Competing interests:** The authors declare that they have no competing interests.

Submitted 19 December 2012
Accepted 11 June 2013
Final Publication 2 July 2013
10.1126/scisignal.2003905
Citation: A. Anisimov, V.-M. Leppänen, D. Tvorogov, G. Zarkada, M. Jeltsch, T. Holopainen, S. Kaijalainen, K. Alitalo, The basis for the distinct biological activities of vascular endothelial growth factor receptor–1 ligands. *Sci. Signal.* **6**, ra52 (2013).